# LEAST-SQUARES DIP ANGLE 4D MIGRATION FOR OBN AND TOWED STREAMER IMAGING

R. Haacke[1], M. Drwila[1], R. Higgins[1], H. Joad[1], S. Knapp[2], C. Schiott[2], C. Hidalgo[3], N. Ahmad[3]

[1] CGG; [2] Hess; [3] INEOS

## Summary

The migrated dip-angle domain provides a powerful opportunity to distinguish 4D noise from signal based on similarity filtering applied to data decomposed by position, frequency, and geological dip. However, 4D signal protection is problematic when the signal itself forms from differences between baseline and monitor. A set of dip-angle similarity filtering methods applied to towed streamer and OBN data from South Arne field show that 4D signal preservation is possible even with strong time-shift signals between baseline and monitor. Signal protection can be achieved with wrap-around time-warping applied within the filtering methods. A better approach detects lack of coherent signal rather than similarity of coherent signal when present. Using this method it is possible to attenuate significant levels of migration noise without appreciably altering the 4D signal. Dip-angle filtering with workflows that preserve surface offset also allow the similarity filtering to be combined with least-squares Kirchhoff migration using single-iteration migration deconvolution. Results show noise attenuation via similarity filtering complementing the illumination compensation achieved by the least-squares method.

# Least-Squares Dip Angle 4D Migration for OBN and Towed Streamer Imaging

## Introduction

Fluid production at the South Arne field (Schiøtt et al., 2008) has led to replacement of oil with water, and compaction of its chalk reservoir. The geophysical change is captured in a time-lapse 4D sense by three towed-streamer surveys and a high-density OBN. In terms of shot and receiver positions, none of the towed streamer datasets has good repeatability (Calvert, 2005) with the OBN. Nevertheless, 4D time-steps between the towed-streamer and OBN acquisitions represent valuable information in geophysical monitoring of the reservoir. This provides motivation to process and image the towed streamer and OBN datasets in a manner that reduces 4D noise while preserving fluid-production signal.

Kirchhoff dip-angle gathers (Audebert et al., 2003) provide a powerful domain in which to identify and remove non-repeatable 4D noise from the seismic image (Haacke et al., 2017). This works particularly well because signal processing takes place prior to completion of the migrated seismic image, which is formed with a final summation across dip-angles. The dip-angle domain allows data to be filtered using decomposition with respect to geological dip, position in the image, and frequency. In the following sections, the method of 4D dip-angle filtering is developed with a range of techniques that identify and remove 4D noise. The discussion focuses on distinguishing 4D noise from 4D signal that, by definition, is produced by differences in the baseline and monitor datasets. Finally, dip-angle processing is combined with least-squares imaging using single-iteration migration deconvolution (Wang et al., 2017). The method is illustrated with results from South Arne, focusing on the 1995 towed-streamer and 2014 OBN pair, and comparing with the 1995 and 2005 towed-streamer pair as a sense check on the result.

## Method

The 1995 towed streamer (TS) survey differs to the 2005 TS survey in both source specification and cable geometry, although nominal tow depths for sources and cables are the same. The surveys were not designed for 4D compatibility. The OBN survey is different again, with receivers on a 25×200 m grid at the seabed, in 50-60 m of water. The datasets were processed independently through 3D denoise, deghosting, designature, and demultiple. After a range of tests for 4D binning, a dSdR cost function was used for the TS datasets, with 90 m threshold used to reject the most different trace pairs. Common offset interpolation and regularisation, including offset and azimuth regularisation terms, then

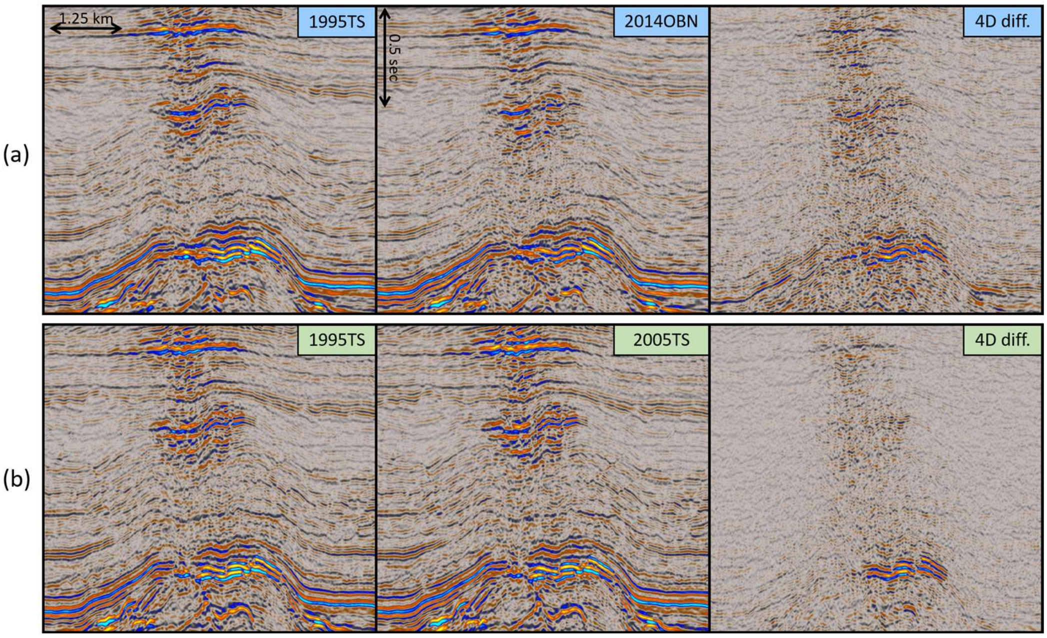

***Figure 1*** *Raw (matched) migration results for: (a) 1995 towed-streamer and 2014 OBN pair; (b) 1995 towed-streamer and 2005 towed-streamer pair. The 4D-difference is baseline–monitor.*

completed the processing flow for input to migration. The relatively large 90 m threshold minimised gaps in the dataset, giving quieter 4D results after regularisation and migration than a smaller threshold that increases trace repeatability at the expense of subsurface coverage. For the TS and OBN pair, 4D binning tests using (i) estimated subsurface reflection point and incidence angle, and (ii) trace cross-correlation, did not improve the results over a surface dSdR cost function, presumably due to the shallow water depth. For simplicity, therefore, 4D binning used dSdR with a 50 m threshold, which is smaller than for the TS pair because of the high OBN shot density on a 50×50 m carpet. Regularisation and interpolation then completed the flow for input to migration. No redatuming of the OBN data was applied prior to migration.

Migration results (Figure 1), with global match filtering of monitor to base, show clear 4D signal at the top chalk reservoir in both 4D pairs, accompanied by incoherent noise and geological leakage strongest in the TS/OBN pair. Much of the energy in the TS/OBN difference is un-cancelled migration noise, and this presents the target for dip-angle image processing. Geological leakage, on the chalk flanks for example, is better treated by improvements in 4D binning and is not addressed by dip-angle processing.

The migrations for all datasets are configured to output dip-angle gathers (geological dip) for each offset class. The final migrated image is produced by summing dip-angle gathers into offset sub-images, then stacking across offset with muting in the usual way. The first similarity-filtering method is a sample-by-sample cross-correlation approach applied in discrete frequency bands. Noise is identified and

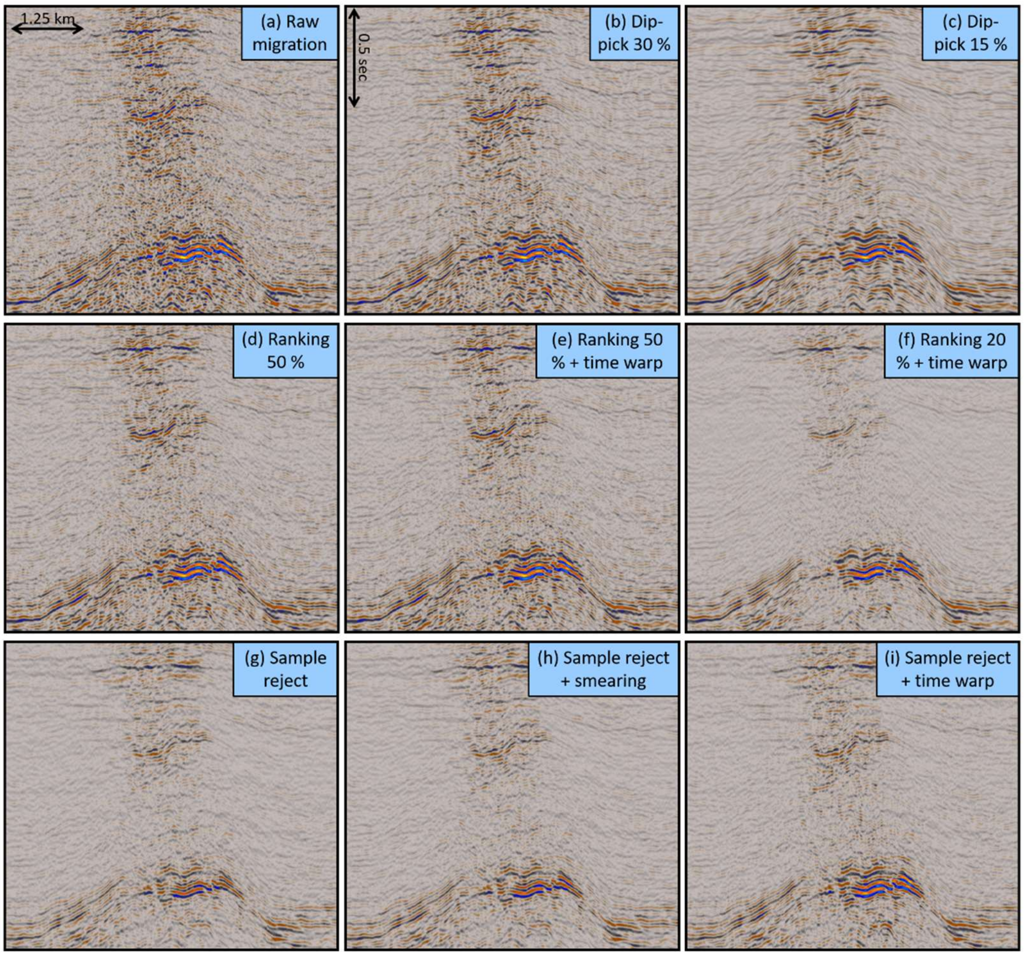

***Figure 2*** *Final stack 4D-differences, 1995TS–2014OBN: (a) Raw migration; (b) dip-pick keeping strongest 30 % of dips; (c) dip-pick keeping strongest 15 % of dips; (d) windowed similarity ranking keeping top 50 % of dips; (e) result (d) with wrap-around time warping; (f) result (d) keeping top 20 % of dips and with wrap-around time warping; (g) sample-by-sample rejection of negative cross-correlation values in octave bands; (h) result (g) with 8 ms vertical smearing; (i) result (g) with wrap-around time warping.*

removed by rejecting samples with negative cross-correlation values. This aggressive method risks damage to signal in the presence of 4D time-shifts, however, so two mitigation strategies are described. The first is to smear the rejection filter vertically by an amount sufficient to cover 4D time-shifts in the data. The second is to apply a wrap-around, reversible, 1D time-warping of the monitor trace to the baseline trace computed after dip-angle summation but applied to dip-angle gathers.

To further protect signals with 4D time-shift, a milder similarity-filtering method is presented in which the dip-angle traces are cross-correlated between baseline and monitor in a running time-window. The dip-angles are then ranked within each time-window and the traces with lowest cross-correlation values are rejected. This windowed similarity ranking approach tends to identify dip-angles with incoherent noise, leaving coherent signals in the angle pass band. This milder method can also be applied with wrap-around time warping, although warping has little impact as the ranking is efficiently detecting the worst of the noise and preserving coherent signal.

The final, and mildest, implementation is to measure the RMS amplitude of dip traces on the baseline in a running time-window, then ranking and picking the strongest dips and applying these as a dip selection for both baseline and monitor. This harmonises the dip content of the two images without measuring similarity between the two.

The filtered dip-angle gathers are then summed across dip to produce offset gathers suitable for single-iteration least-squares migration, in which the filtered data are demigrated and remigrated. The

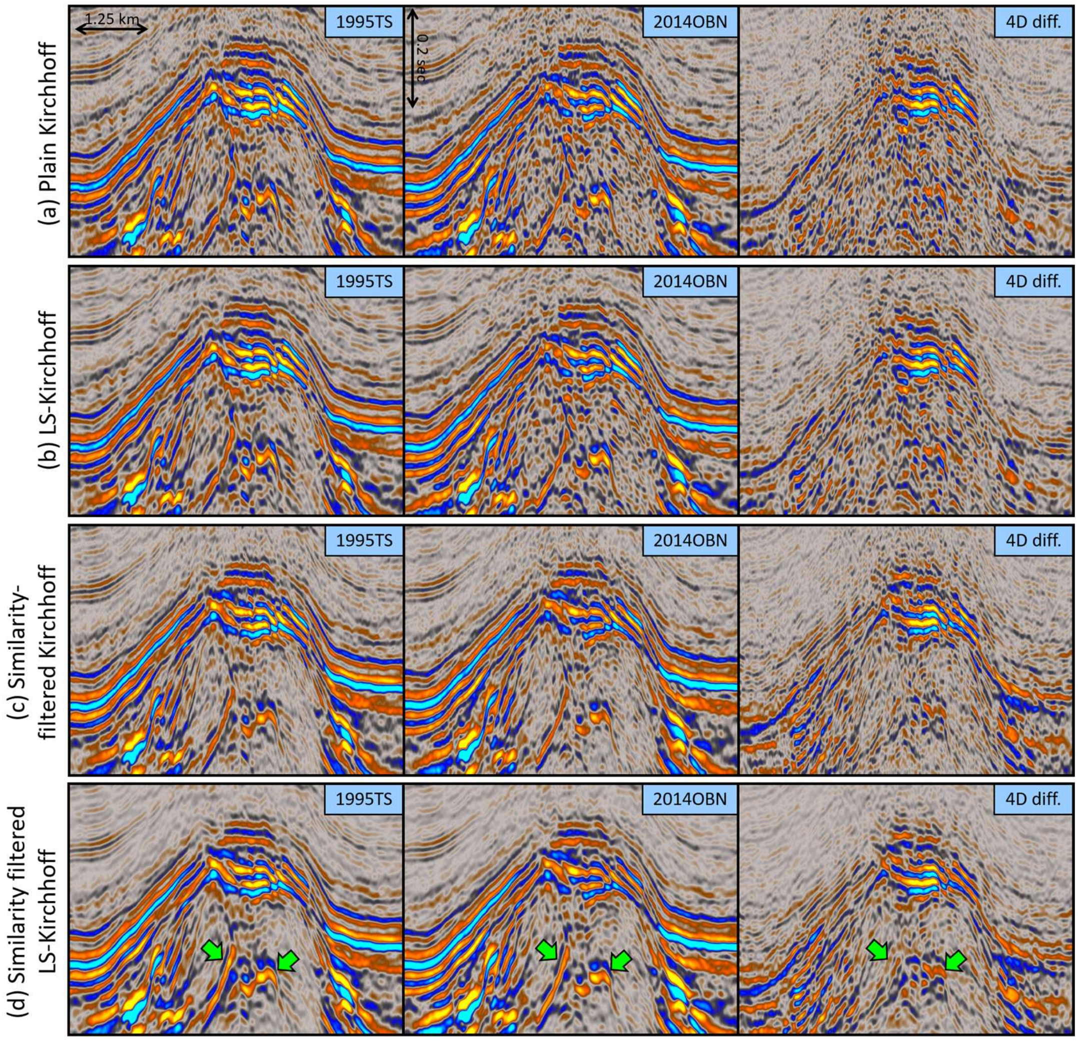

***Figure 3*** *Final stacks of the 1995TS baseline, 2014OBN monitor, and 4D-differences (1995TS–2014OBN) for: (a) Plain Kirchhoff; (b) LS-Kirchhoff; (c) Similarity-filtered plain Kirchhoff; (d) similarity-filtered LS-Kirchhoff with base-chalk illumination improvements (green arrows).*

remigration and the first migration after similarity filtering are used to compute a curvelet-domain Hessian filter that further removes migration noise and corrects amplitude for variable illumination.

## Results

Final stacks, Figure 2, show the relative severity of the different methods in attenuating noise and preserving 4D signal. The mildest result (Figure 2b) comes from picking the top 30 % of strongest dips on the baseline and applying the dip selection to base and monitor. A stronger parameterisation (Figure 2c, picking the top 15 % of strongest dips) removes cross-cutting noise while preserving coherent signal. Keeping the top 50 % of dips in the windowed similarity ranking method (Figure 2d) seems to remove more noise than the dip-picking method while preserving signal at a similar level. Wrap-around time warping (Figure 2e) makes little impact on this result as the signal preservation is already good. A stronger parameterisation keeping the top 20 % of dips (Figure 2f) is therefore tolerable. In contrast, the sample-by-sample filtering (Figure 2g) is an aggressive method that removes significant noise but also damages the 4D signal, which in this case has an appreciable 4D time-shift between baseline and monitor. Vertical filter smearing over 8 ms (Figure 2h) improves signal protection for this method, with further improvement achieved using wrap-around time warping (Figure 2i). Comparison to the difference of 1995 TS and 2005 TS data (Figure 1b) suggests good signal preservation, although with geological leakage present in the TS/OBN pair that may be addressed by improvements in 4D binning.

The windowed similarity ranking result in Figure 2e (representing a good but conservative result with some residual noise) was then carried forward into single-iteration least-squares (LS) Kirchhoff migration, Figure 3. Compared with plain Kirchhoff, the LS flow removes some high frequency noise (Figure 3a & 3b) but the effect of illumination compensation is hard to see due to noise in the 4D difference. The similarity-filter removes sufficient noise that illumination compensation in the LS flow is more clearly visible (Figure 3c & 3d, green arrows), particularly toward the base of the chalk.

## Conclusions

Migration noise can be attenuated successfully in the dip-angle domain, but care must be taken to protect 4D signal that by definition is different in baseline and monitor. Mild approaches use dip-selection based only on one vintage and thus do not require similarity between 4D signals. Filtering based on similarity between baseline and monitor can also be done safely if the emphasis is on detection of incoherent noise rather than similarity of coherent signals. In this way, windowed cross-correlation ranking and rejection of the least similar traces preserves signal even with strong 4D time-shift between baseline and monitor. Combined similarity-filtering and least-squares Kirchhoff migration allows the similarity filter to remove strong migration noise while the least-squares corrects for variations in illumination.

## Acknowledgements

We thank Hess, INEOS, Danoil and CGG for permission to publish.

## References

Audebert, F., Froidevaux, P., Nicoletis, L. and Rakotoarisoa, H. [2003] Migration in the angle domain, an inside view. *65th EAGE Conference & Exhibition*, Stavanger, Expanded Abstracts.
Calvert, R. [2005] Insights and methods for 4D reservoir monitoring and characterization. *Distinguished Instructor Short Course*, **8**, *Society of Exploration Geophysicists*.
Haacke, R. R., Casasanta, L., Hou, S., Henderson, J. R. [2017] Dip-angle image filtering for 4D processing of towed-streamer and OBN datasets. *First EAGE Workshop on Practical Reservoir Monitoring, Amsterdam.*
Schiøtt, C. R., Bertrand-Biran, V., Hansen, H. J., Koutsabeloulis, N. and Westeng, K. [2008] Timelapse inversion and geomechanical modelling of the South Arne field. *First Break*, **26**, 85-91.
Wang, P., Huang, S., Wang, M. [2017] Improved subsalt images with least-squares reverse time migration. *Interpretation*, **5**, dx.doi.org/10.1190/INT-2016-0203.1